Journal of Applied Polymer Science

Electron Beam and UV Cationic Polymerization of Glycidyl Ethers – PART I: Reaction of Monofunctional Phenyl Glycidyl Ether

Matteo Mascioni,[1] Narendra N. Ghosh,[1,2] James M. Sands,[3] Giuseppe R. Palmese[1]

[1]Department of Chemical and Biological Engineering, Drexel University, Philadelphia, Pennsylvania 19104

[2]Department of Chemistry, Birla Institute of Technology and Science Pilani, KK Birla Goa Campus, Zuarinagar, Goa 403726, India

[3]Materials and Manufacturing Sciences Division, US Army Research Laboratory, Aberdeen Proving Ground Maryland 21005

Correspondence to: G. R. Palmese (E-mail: grp27@drexel.edu)

ABSTRACT: Investigations of electron beam (e-beam) and ultra violet (UV)-induced cationic polymerization kinetics of a mono-functional epoxy system, phenyl glycidyl ether (PGE), were conducted using real time *in situ* near infrared (NIR) spectroscopy. Effects of processing variables such as temperature and dose rate on initiation and propagation rate constants have been assessed. The experimental results and results from a simple mathematical model developed to predict the reaction behavior under continuous irradiation showed very good agreement. This work provides a basis for investigating the cure behavior of more complex and industrially relevant crosslinking epoxy systems where diffusion limitations play an important role as discussed in PART II. © 2013 Wiley Periodicals, Inc. J. Appl. Polym. Sci. 130: 479–486, 2013

KEYWORDS: kinetics; photopolymerization; ring-opening polymerization; spectroscopy

Received 22 August 2012; accepted 12 February 2013; published online 19 March 2013
DOI: 10.1002/app.39184

INTRODUCTION

Polymers cured by radiation such as ultra violet (UV) or electron beam (e-beam) have a wide range of applications including coatings, inks, adhesives, and composite materials. Radiation curing offers significant advantages over traditional thermal curing. These include shorter curing times, lower curing temperature, reduced VOC emissions, lower energy consumption, and reduced overall manufacturing costs. Particularly because of the potential for lower residual cure and thermal stresses e-beam processing allows for the use of low cost fabrication tools made from lower-cost reusable or disposable materials. Compared to UV curing that can generally only be used for thin and transparent materials, high-energy e-beams can be used to cure thick-section composite materials. Over the past several years, e-beam curing has been actively explored as a means to reduce the processing and fabrication costs of complex structures including fixed-winged and rotor aircraft, ground vehicles and spacecraft. Despite good thermal properties and significant processing advantages, epoxy-based composites manufactured using radiation curing exhibit low compressive strength, poor interlaminar shear strength, and low fracture toughness.[1–14] To properly address the shortcomings associated with the radiation curable epoxy system, many aspects of the cure process such as chemical kinetics and the influence of processing conditions on the final material properties must be well understood.[13,14]

Thermal curing of epoxy resins by cationic polymerization has been investigated by a number of researchers.[15–17] Boron trifluoride amine (BF_3-amine) complexes are often employed as initiators of cationic polymerization. The mechanisms associated with cationic polymerization initiated by BF_3-amine catalysts have been reported by Chabanne et al.[18] and Matejka et al.[19,20] The cationic polymerization of these systems is akin to radiation-induced polymerization and understanding the polymerization of these systems provides a basis for investigating radiation-induced cationic polymerization of epoxy resins. Epoxides polymerize cationically in presence of appropriate photo-initiator under e-beam irradiation. Crivello and coworkers[21–24] have reported that several onium salts, e.g. diaryliodonium salts, triarylsulfonium salts and phenacylsulfonium salts serve as cationic photo-initiators.

Several efforts have been made to analyze and model the kinetic of radiation-induced cationic polymerizations. Ionescu-Vasii et al.[25] have reported a photo-calorimetric approach to study the photo-induced cationic polymerization of phenyl glycidyl ether (PGE) in the presence of an iodonium salt and derived a model for the reaction. They have proposed a model to predict the concentration of PGE as a function of time that involves (i) an initiation constant (representative of the formation of cationic active centers), (ii) propagation constant (representative of the disappearance of epoxy monomer over time) and (iii) a

parameter β. Timpe and Rajendran[26] have reported a model for the polymerization of PGE induced by UV radiation that includes a termination constant to account for potential deactivation of cationic active centers and a quantum yield (or initiation efficiency), which was found to be dependent on the specific sensitizer used in the system. However, to the best of our knowledge, an *in situ* study on assessment of the dependency of epoxy polymerization kinetics linking processing parameters to initiation and propagation rate constants has not yet been reported.

In this article we present an investigation of the kinetics of UV and e-beam-induced cationic polymerization of a mono-epoxy system, phenyl glycidyl ether (PGE), by using a real time *in situ* near infrared (NIR) spectroscopy technique developed and reported on earlier by our group.[12] In the earlier report broad observations of conversion based on limited data were presented. Herein we report new polymerization data as well as detailed kinetic analysis and model development for cationic polymerization of mono functional epoxies under continuous UV and e-beam irradiation. The analysis and the resulting conclusions are used as a starting point in the development of a kinetic model describing diffusion limited polymerization of difunctional epoxies described in Part 2 of this work. A number of investigations of e-beam curing of epoxy resins have used Fourier transfer infrared (FTIR) and differential scanning calorimetry (DSC)[27–31] to follow cure process *ex situ*. The results of these studies are affected by the presence of rapid dark reactions that occur when temperature quenching is used. An advantageous aspect of this work is that *in situ* NIR spectroscopy was used to investigate the kinetics of e-beam-induced epoxy polymerization avoiding the need for time-interrupted experiments.

PGE was chosen as a model epoxy system because it contains only one epoxy group per molecule and polymerizes to linear chain products, thus avoiding diffusion limitation associated with gelation and vitrification of cross linked networked polymers (e.g., diglycidyl ether of bisphenol A). As both UV and e-beam-induced polymerization of PGE proceed via cationic polymerization mechanism, UV-induced polymerization of PGE has been investigated first to develop model rate equations and values of initiation and propagation specific rate constants (k_i and k_p) of the reaction. This is followed with the investigation of e-beam-induced polymerization of PGE. In both cases the effects of processing variables (e.g., temperature, radiation intensity, and photo-initiator concentration) on k_i and k_p are reported. The experimental conditions were selected to provide a range of temperature, photoinitiator concentration, and irradiation intensity that is typical of what is used in the processing of such materials.

EXPERIMENTAL

Materials

In this study, the chemicals used were phenyl glycidyl ether (PGE) (Aldrich Chemical Company, St. Louis, MO) and CD-1012 (UCB Radcure, Louisville, KY) a diaryliodonium hexafluoroantimonate salt, as photo-initiator. Figure 1 shows the chemical structures of PGE and CD-1012. PGE was dried using 4 Å molecular sieves (Aldrich Chemical Company, USA) in order to limit the water concentration to below 0.1% in the reactant. The sieves were activated at 175°C for 12 h prior to use. Drying of PGE was important because it has been observed that the presence of water significantly influences radiation-induced cationic polymerization of epoxy.[11]

Material	Chemical Structure
Phenyl glycidyl ether (PGE)	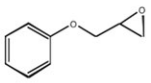
Diphenyl iodonium hexafluoroantimonate	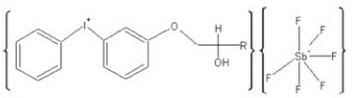

Figure 1. Materials used in the experimental work.

Real Time *In Situ* Near IR Spectroscopy Apparatus

An *in situ* real time near infrared (NIR) spectroscopy technique was developed to monitor the reaction kinetics of UV and e-beam-induced cationic polymerization of PGE.[12] The experimental apparatus consisted of a NIR spectrometer (Control Development, South Bend IN), a temperature controller, a UV source and a custom made sample chamber and holder. The NIR spectrometer has a spectral range from 1160 to 2250 nm with a resolution of 4 nm at a spectral collection rate of one per 0.166 s. To ensure proper transmission of the infrared light in the whole range of interest, custom-made low-hydroxyl silica fiber optic cables (Thorlabs, Newtown, NJ) were used. The specific fibers used in this work have a numerical aperture of 0.22, a nominal diameter for the silica core of 200 nm, a primary fluorine-doped silica cladding with a diameter of 240 μm and an external buffer diameter of 400 μm. The near infrared probe light was produced by a white light source transmitted through an optical link that collimates the light into a focused beam. The focused beam passed through the sample and was subsequently collected by a focusing lens that passed the light to the spectrometer through the fiber optic cable.

UV Irradiation

The UV light source used in this study was a Novacure™ (EFOS, Mississauga, ON, Canada). It consisted of three main components: a 100 W mercury vapor short arc ultra-violet lamp, a set of quartz fiber light guides and a UV light band pass filter that cuts off light below 300 nm wavelength and above 500 nm wavelength. Approximately 40% of the output energy is for wavelengths between 350 nm and 400 nm, 40% is for wavelengths between 400 nm and 500 nm, and 20% for wavelengths between 300 and 350 nm. Diffusers were used to control UV light intensity below 100 mW/cm^2. The overall light intensity was measured using a differential scanning calorimeter equipped with black carbon disks that absorb the UV radiation. More details of these procedures are given elsewhere.[32]

Mixtures of PGE and CD-1012 were placed in a custom-made sample holder. The sample holder was an aluminum block,

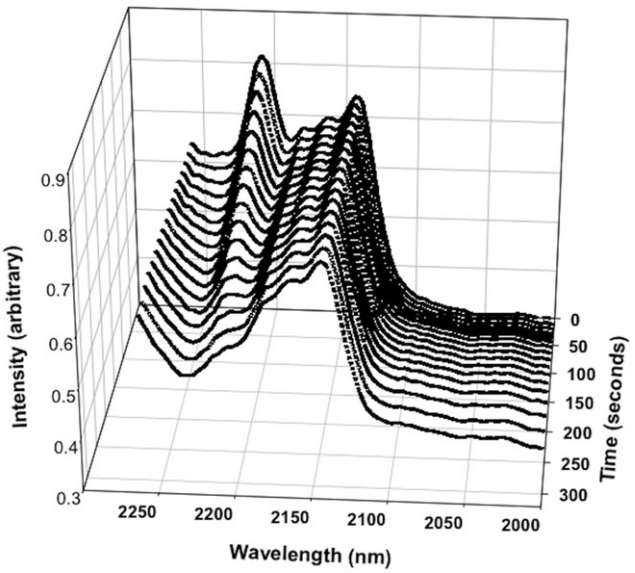

Figure 2. Typical real time NIR spectra obtained for UV-induced cationic polymerization of dry PGE at 70°C. Photo-initiator concentration and UV Intensity were 0.44 wt % and 15.90 mW/cm^2, respectively. Time interval between spectra was 20 s.

which was mounted on a chill plate and was equipped with cartridge heaters for temperature control. The path length of the infrared light through the resin sample was 1.6 ± 0.03 mm. UV light impinged the sample in a direction perpendicular to the infrared light. The sample thickness in the direction of UV radiation varied between 0.60 to 0.65 mm. All experiments were conducted in such a way that at least 90% of 365 nm wave length UV light could pass through the sample. The typical size of the sample was 0.6 mm × 1.6 mm × 3.0 mm.

E-Beam Irradiation

The e-beam cure experiments were performed using a linear accelerator (LINAC) at the Boeing Radiation Effects Laboratory (Seattle, WA). The LINAC is a uniquely designed accelerator unit that has a maximum operational power of 1.0 kW. The LINAC was tuned for 10 MeV electrons. The scan rate was 0.3 Hz and the pulse repetition frequency was 15 Hz. Samples were centered within the beam scan path. In order to avoid changing beam characteristics, the dose rate was varied by changing the pulse width of the beam from 2.5 to 10 μs, and by moving the sample vertical position relative to beam source. Film dosimetry was used to confirm delivered doses for all configurations. For the experiments reported herein a total dose of 50 kGy was delivered to the samples without interruption.

Determination of Epoxy Conversion

The kinetics of the UV and e-beam-induced cationic polymerization of PGE was determined by monitoring the disappearance of NIR peak at 2209 nm (which is the characteristic of epoxy group) versus time.[12] Figure 2 represents typical real time NIR spectra, which shows the disappearance of epoxy peak of PGE with time upon UV irradiation. A number of experiments using *in situ* NIR were conducted varying photo-initiator concentration, UV light intensity, e-beam dose rate and temperature.

The spectra were analyzed by calculating the ratio between the epoxy characteristic peak height at a given time and the peak height at time $t = 0$, defined as the instant when the UV light or e-beam was turned on. This procedure was based upon the assumption of a linear relationship between the characteristic peak height and the concentration of epoxy functional groups. This assumption was tested with a concentration versus epoxy peak height calibration procedure, in which measured amounts of PGE were mixed with known amounts of poly-PGE and a linear behavior of the concentration versus mole (or weight) fraction of PGE was observed.[12]

RESULTS AND DISCUSSION

Rate Equations Used to Determine Rate Constants

The overall reaction mechanism of UV and e-beam radiation-induced cationic polymerization of epoxy consists of two important steps. The initiation step involves the photo-decomposition of a photo-initiator molecule to yield a positively charged species (typically a proton H^+). The proton thus formed readily reacts with an epoxy functional group to form an active center ($H\text{-}M^+$). The following step is the propagation step, which consists of typical cationic chain propagation. In the absence of chemical species, that are capable of deactivating the cationic active centers (such as amines and other nucleophiles), termination reactions are not expected and a living polymerization can in principle be achieved.

The initiation reaction that leads to the formation of a proton from a diaryliodonium salt molecule upon UV or e-beam exposure was assumed to proceed as follows:

$$C + h\nu \rightarrow H^+ + X \quad (1)$$

$$H^+ + M \rightarrow H - M^+ \quad (2)$$

here, C represents the photo-initiator present in the system at a given time, hν refers to a photon of the irradiating light, M refers to the epoxy monomer, and X is a mixture of initiation products that doesn't take part directly in the subsequent polymerization reactions. Equation (1) summarizes a series of reactions, by which one diaryliodonium salt molecule reacts due to UV or e-beam radiation to yield the hydronium ion. Equation (2) represents the formation of an epoxide active center ($H\text{-}M^+$) that initiates the polymerization.

The decomposition of the photo-initiator and formation of active centers was modeled based on the following assumptions: (i) at most one active center forms from a single initiator molecule, (ii) the reaction represented by eq. (2) is much faster compared with the reaction in eq. (1), i.e. once the hydronium ion has been formed, its reaction to yield an epoxide active center is instantaneous and, (iii) the average lifetime of a cationic active center is much longer than the time required for the polymerization to complete. In other words, within the magnitude of the time scales considered in this work, no deactivation of the cationic active centers occurs over time.

Applied Polymer SCIENCE

The initiation reaction can be assumed to be first order with respect to the concentration of photo-initiator. The concentration of initiator at a given time can be expressed as:

$$C(t) = C_o - I \tag{3}$$

where I is the concentration of cationic active centers (i.e., H^+ ions or PGE oligomer and polymer chains positively charged at one end) and C_o is the initial concentration of photo-initiator. The formation of active centers is assumed to follow first order kinetics so that Equation (4) describes the concentration of active centers with respect to time (t) upon irradiation where k_i is known to depend on photoinitiator type, irradiation intensity, and efficiency.

$$I(t) = C_o \cdot [1 - \exp(-k_i \cdot t)] \tag{4}$$

Propagation in such cationic polymerization is known to proceed via two competing mechanisms known as the activated chain end (ACE) and activated monomer (AM)[18–20] as shown below by reactions (A) and (B):

Activated Chain End (ACE) mechanism:

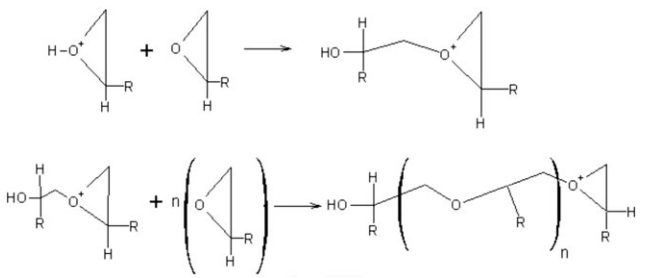

(A)

Activated Monomer (AM) mechanism:

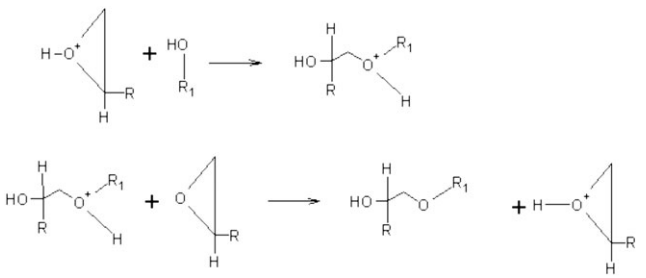

(B)

In ACE, growing chain cyclic tertiary oxonium ions are formed and polymerization proceeds by chain addition of monomer. On the other hand, AM mechanism proceeds via the addition of molecules containing hydroxyl groups to the activated monomer. This is accompanied by a charge transfer that regenerates H-M$^+$. During the initial stages of reaction and in systems with low initial concentration of hydroxyl groups, ACE mechanism is predominant. However, the presence of hydroxyl groups, i.e., water, alcohol, polymer chain ends and co-monomer, can favor the AM mechanism.[11]

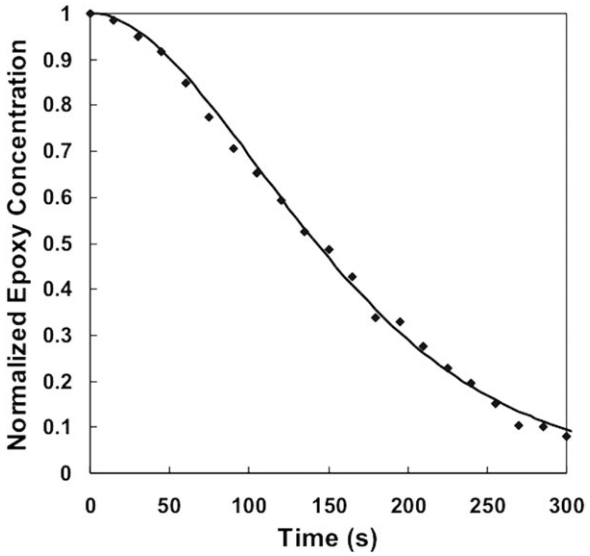

Figure 3. Comparison between experimental data (●) and model predictions for PGE (UV light intensity = 47.7 mW/cm^2, temperature = 60°C and initiator concentration = 0.44 wt %, k_i = 0.00182 s^{-1}, k_p = 4.11 L mol^{-1} s^{-1}).

Because the experiments were performed in dry condition, propagation is expected to follow the ACE mechanism. As also done by others,[25] the propagation reaction may be expressed by a second order rate expression;

$$dM/dt = -k_p \cdot M \cdot I \tag{5}$$

where M is the concentration of monomer, I is the concentration of cationic active centers and k_p is the specific polymerization rate constant. From eqs. (4) and (5) the rate equation for propagation can be obtained as follows:

$$\frac{M}{M_o} = \exp\{-k_p \cdot C_o \cdot t + \frac{k_p}{k_i} \cdot C_o \cdot [1 - \exp(-k_i \cdot t)]\} \tag{6}$$

In eq. (6) the value of M/M_0 can be determined experimentally from the ratio between the epoxy peak height at a given time and the one at $t = 0$ in the NIR spectra of the samples. Since C_o can be calculated, the model above has two unknown parameters k_i and k_p. An iterative spreadsheet-based fitting program was created in order to obtain numerical values for the model parameters k_p and k_i for each experimental run. The fit was performed using a least-squares analysis, in which the sum of the squared errors between each data point and the value predicted by eq. (6) was minimized. A representative plot that illustrates the comparison of experimental data and model predictions based on fitted parameters is shown in Figure 3.

For all the experiments conducted in this work, the maximum discrepancy between the conversion data and the model predictions was found to be less than 3% conversion. The fitted

Table I. Experimental Consistency and Error for the Kinetic Parameters Obtained from Two Different Experiments

Run	k_i[a]	k_p[a]	R^{2a}	k_i[b]	k_p[b]	R^{2b}
1	0.0047	2.15	0.991	0.00165	4.39	0.994
2	0.0056	2.26	0.991	0.00176	4.06	0.990
3	0.0051	2.43	0.996	0.00161	4.09	0.990
Average	0.0051	2.28		0.00167	4.18	
Standard Deviation	0.00045	0.14106		0.00007	0.182	
Error%	8.78	6.19		4.64	4.37	

[a]Experiments were performed at 60°C.
[b]Experiments were performed at 70°C.UV light intensity = 44.52 mW/cm^2 and photo-initiator concentration = 0.44 wt % for all experiments.

curves based on the kinetic model accurately represent experimental concentration data in the entire range of conversions. The quality of the plot was quantified using a coefficient of correlation R^2 defined as:

$$R^2 = \left[1 - \sum_1^m \frac{(y_i - Y_i)^2}{(Y_i - Y_{mean})^2}\right]^2 \quad (7)$$

where, Y_i refers to the experimental data points, y_i to the model predictions, Y_{mean} is the average value of Y and m is the number of data points. A value of 1 for the parameter R^2 implies a perfect match between data and fit. For all cases $R^2 > 0.99$.

Experimental variability was determined by using multiple experiments for a given set of conditions. The standard deviation was used as an indication of how the experimental variability affects the calculated values of the kinetic parameters k_i and k_p. Two experimental conditions were used and for each condition three experimental runs were performed. The data were fitted to the kinetic model and the corresponding kinetic parameters calculated. The results of such experiments are summarized in Table I and a representative plot is shown in Figure 4. It was observed that the error associated with the experimental reproducibility was larger than the one associated with the fit quality and is therefore expected to have a greater effect on calculated k_i and k_p parameters.

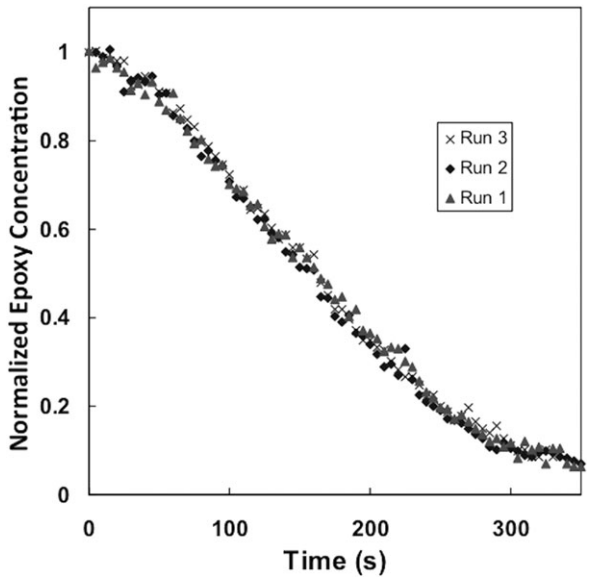

Figure 4. Plot showing experimental consistency (temperature = 60°C, UV intensity = 45.43 mW/cm^2 and initiator concentration = 0.44 wt %).

Effect of Photo-Initiator Concentration

The effect of photo-initiator concentration on rate constants (k_i and k_p) was determined by performing experiments with various photo-initiator concentrations up to 3 wt %. For UV polymerization experiments were conducted at 70°C with light intensity of 15.90 mW/cm^2. E-beam experiments were conducted at 50°C using a dose rate of 3750 rad/s. The values of rate constants are listed in Tables II and III for UV and e-beam-induced polymerization respectively. It was observed that, within the bounds of experimental variability both k_i and k_p values are practically independent of initiator concentration. This observation suggests that the initiation reaction follows first order rate equation well.

Effect of UV Light Intensity and e-Beam Dose Rate

To evaluate the effect of UV light intensity and e-beam on the kinetics of cationic polymerization of PGE, the reactions were performed with various UV intensities (ranging from 5.3 to 53 mW/ cm^2) and e-beam dose rates varying between 3750 to 26100 rad/s. In case of UV-induced reactions photo initiator concentration was 0.44 wt % and temperature was 60°C. E-beam experiments were performed using 1 wt % photo-initiator concentration at 50°C. It was observed the k_i is strongly dependent on UV light intensity and e-beam dose rate because the formation of cationic active centers (H-M$^+$) is directly proportional to the UV light intensity and e-beam dose rate. In contrast, k_p was found to be independent on UV light intensity or e-beam dose rate. Figures 5(a,b) show the linear behavior of

Table II. Effect of Photo-Initiator Concentration on k_i and k_p on UV-Induced Polymerization of PGE

Photo-initiator concentration (wt %)	k_i (s^{-1})	k_p (L mol^{-1} s^{-1})
0.44	0.00182	4.11
0.66	0.00205	4.20
0.94	0.00190	4.35

All reactions were performed at 70°C and UV light intensity 15.90 mW/cm^2.

Table III. Effect of Photo-Initiator Concentration on k_i and k_p on e-Beam-Induced Polymerization of PGE

Photo-initiator concentration (wt %)	k_i (s^{-1})	k_p (L mol^{-1} s^{-1})
0.5	0.00080	0.701
1	0.00098	0.892
3	0.00095	0.873

All reactions were performed at 50°C and E-beam dose rate 3750 Rad/s.

Table IV. Effect of UV Light Intensity on k_i and k_p on UV-Induced Polymerization of PGE

UV light intensity (mW/cm^2)	k_i (s^{-1})	k_p (L mol^{-1} s^{-1})
5.3	0.00041	2.14
15.9	0.00167 ± 0.000077	2.11 ± 0.14
26.5	0.0034	2.37
47.7	0.0063	2.25
58.3	0.0069	2.40

All reactions were performed at 60°C and photo-initiator concentration 0. 44 wt %.

Table V. Effect of e-Beam Dose Rate on k_i and k_p on e-Beam-Induced Polymerization of PGE

E-beam dose rate (Rad/s)	k_i (s^{-1})	k_p (L mol^{-1} s^{-1})
3750	0.00098	0.892
6525	0.0020	0.966
7500	0.0023	0.939
10000	0.0040	0.978
15000	0.0047	0.870
26100	0.0090	0.969

All reactions were performed at 50°C and photo-initiator concentration 1 wt %.

k_i as a function of UV light intensity and e-beam dose rate intensity respectively. Tables IV and V summarize the values of k_i and k_p, obtained due to variation of UV light intensity and e-beam dose rate respectively.

Effect of Temperature

UV-induced polymerization reactions were conducted at various temperatures ranging from 40 to 90°C with constant photo-initiator concentration of 0.44 wt % and UV light intensity 15.9 mW/cm^2 for all cases. It was observed that k_i is independent on temperature and k_p is strongly temperature-dependent (Table VI). Since the UV light is known not to take part directly in the propagation reaction once the cationic active centers are formed, it is reasonable to assume that k_p is independent of either photo-initiator concentration or light intensity, but as any reaction rate constant, strongly dependent on temperature. An Arrhenius-type dependence on temperature was used to fit the rate constant data:

$$k_p = k_{po} \cdot \exp(-E/RT) \quad (8)$$

where T is the reaction temperature (in K), $R = 8.314$ J/(gmol K) is the ideal gas constant, E is the activation energy expressed in kJ mol^{-1} and k_{po} is pre-exponential factor. Figure 6 is the ln k_p versus $1/T$ plot showing a good Arrhenius fit. From analysis of k_p versus temperature data, the Arrhenius parameters k_{po} and E for the propagation reaction were found to be 2.027×10^{11} L mol^{-1} s^{-1} and 70.152 kJ mol^{-1} respectively. Propagation rate constants for e-beam-induced polymerization will be discussed in Part 2 of this work.[33] These have also been found to follow Arrhenius behavior matching UV values closely.

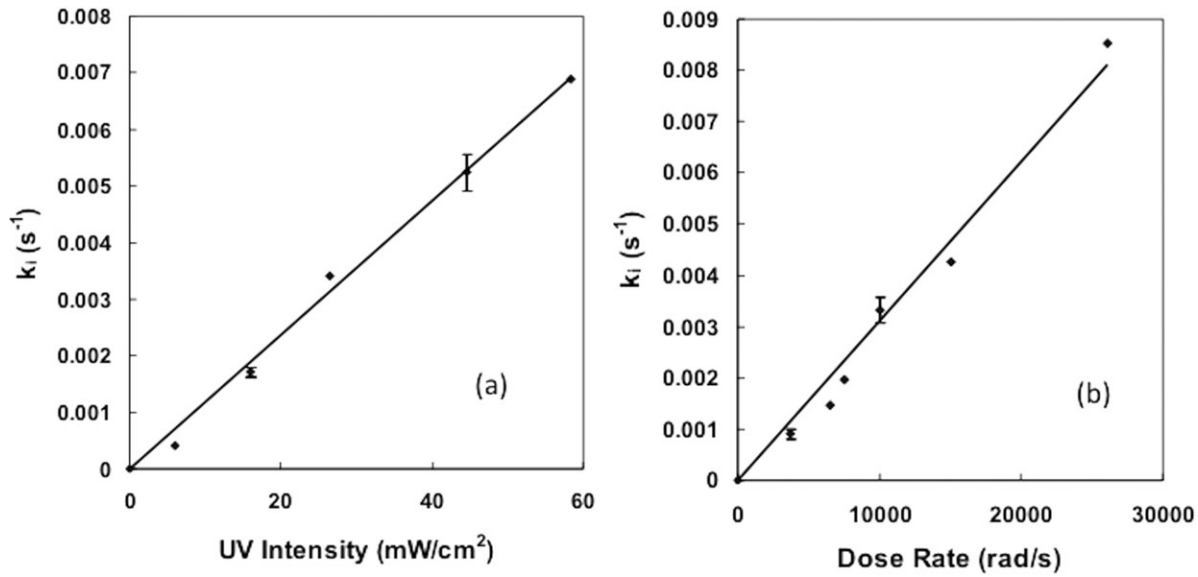

Figure 5. Plots show the dependence of the initiation rate constant (k_i) on (a) UV light intensity and (b) e-beam dose rate.

Table VI. Effect of Temperature on k_i and k_p for UV-Induced Polymerization of PGE

Temperature (°C)	k_i (s^{-1})	k_p (L mol^{-1} s^{-1})
40	0.00174	0.22
50	0.00159	0.80
60	0.00167 ± 0.000077	2.11 ± 0.14
70	0.00182	4.11 ± 0.18
80	0.00180	8.14
90	0.00179	12.5

All reactions were performed with photo-initiator concentration 0.44 wt % and UV light intensity 15.90 mW/cm^2.

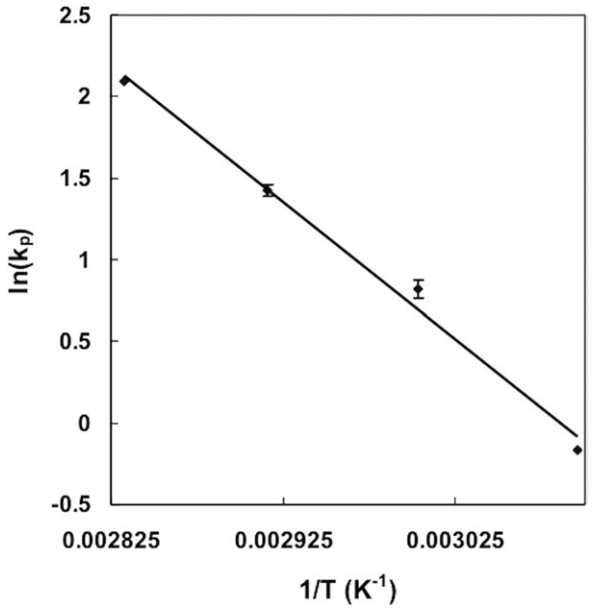

Figure 6. Arrhenius plot for the propagation reaction of UV-induced cationic polymerization of PGE.

CONCLUSIONS

Reaction studies of UV and e-beam-induced cationic polymerization of phenyl glycidyl ether have been reported and a mathematical model has been developed to accurately describe the reaction behavior. The effects of processing parameters on the rate constants of the reaction have been assessed. These parameters include temperature, UV light intensity, e-beam dose rate and photo-initiator concentration. It has been observed that the initiation rate constant (k_i) is dependent on UV light intensity or e-beam dose rate but independent of photo-initiator concentration and temperature. On the other hand, the propagation rate constant (k_p) is dependent on temperature but independent on UV light intensity or e-beam dose rate, and photo-initiator concentration. The mathematical model proposed in this paper showed very good agreement between experimentally obtained and theoretically predicted data. Using these results as a starting point, in Part 2 of this work, UV- and electron beam-induced cationic polymerization kinetics of the industrially relevant difunctional epoxy system diglycidyl ether of bisphenol A (DGEBA) will be reported along with appropriate modifications to the present model allowing for the prediction of diffusion limited behavior associated with vitrification.

ACKNOWLEDGMENTS

The authors gratefully acknowledge the support of Dr. Mark Wilenski and Mr. James Beymer of the Boeing Company for providing support for the e-beam irradiation and measurements and financial support from U.S. Army Research Laboratory (ARL) and Strategic Environmental Research and Development Program (SERDP) "Non Polluting Composites Repair and Remanufacturing For Military Applications – PP1109". NN Ghosh is thankful to BITS Pilani for granting sabbatical leave.

REFERENCES

1. Davidson, S. R.; Wilkinson, S. A. *J. Photoch. Photobio. A.* **1991**, *58*, 123.
2. Saunders, C.; Lopata, V.; Barnard, J.; Stepanik, T. *Rad. Phys. Chem.* **2000**, *57*, 441.
3. Lopata, V. J.; Saunders C. B.; Singh, A.; Janke, C. J.; Wrenn, G.E.; Havens, S. J. *Rad. Phys. Chem.* **1999**, *56*, 405.
4. Rajagopalan, G.; Gillespie, J. W.; McKnight, S. H. *Polymer* **2000**, *41*, 7723.
5. Scranton, A. B.; Baikerikar, K. K. *Polymer* **2001**, *42*, 431.
6. Goodman, D. L.; Palmese, G. R. In Handbook of Polymer Blends and Composites; Kulshreshtha, A.; Vasile, C., Editors; Rapra Technology Ltd Publisher, Shropshire UK, **2002**, p 459.
7. Janke, C. J.; Norris, R.E.; Yarborough, K.; Havens S. J.; Lopata, V. J. In Proceedings of the 42nd International SAMPE Symposium, Society for the Advancement of Material and Process Engineering, USA, **1997**, p 477.
8. Janke, C. J.; Dorsey, G. F.; Havens, S. J.; Lopata, V. J. US patent 5726216, **1998**.
9. Guasti, F.; Rosi, E. *Compos. Part A- Appl S.* **1997**, *28*, 965.
10. Ghosh, N. N.; Palmese, G. R. *Bul. Mater. Sci.* **2005**, *28*, 603.
11. Mascioni, M.; Sands, J. M.; Palmese, G. R. *Nucl. Instrum. Meth. B.* **2003**, *208*, 353.
12. Durmaz, Y. Y.; Sangermano, M.; Yagci, Y. *J. Polym. Sci., Part A: Polym. Chem.* **2010**, *48*, 2862.
13. Ranoux G.; Molinari M.; Coqueret X. *Radiat. Phys. Chem.* **2012**, *91*, 1297.
14. Raghavan J. *Compos. Part A* **2009**, *40*, 300.
15. Bednarek, M.; Kubisa, P.; Penczek, S. *Makromol. Chem. Suppl.* **1989**, *15*, 49.
16. Bednarek, M.; Biedron, T.; Szymanski, R.; Kubisa, P.; Penczek, S. *Makromol. Chem-M Symp.* **1991**, *42/43*, 475.
17. Bouillon, N.; Pascault, J. P.; Tighzert, L. *Makromolekul. Chem.* **1990**, *191*, 1403.
18. Chabanne, P.; Tighzert, L.; Pascault, J. P. *J. Appl. Polym. Sci.* **1994**, *53*, 769.
19. Matejka, L.; Chabanne, P.; Tighzert, L.; Pascault, J. P. *J. Polym. Sci. Polym. Chem.* **1994**, *32*, 1447.

20. Matejka, L.; Chabanne, P.; Tighzert, L.; Pascault, J. P. *J. Polym. Sci. Polym. Chem.* **1997**, *35*, 651.

21. Crivello, J. V. *Nucl. Instrum. Meth. B.* **1999**, *151*, 8.

22. Crivello, J. V.; Fan, M.; Bi, D. *J. Appl. Polym. Sci.* **1992**, *44*, 9.

23. Crivello, J. V.; Lam, J. H. W. *Macromolecules* **1977**, *10*, 1307.

24. Fouassir, J. P.; Burr, D.; Crivello, J. V. *JMS-Pure Appl. Chem. A.* **1994**, *31*, 677.

25. Ionescu-Vasii, L. L.; Dimonie, M. D.; Abadie, M. J M. *Polym. Int.* **1998**, *47*, 221.

26. Raejendran, A. G.; Timpe, H. J. *J. Polym. Sci. Polym. Chem.* **1991**, *29*, 1491.

27. Ribeiro, R.; Morgan, R. J.; Bonnaud, L.; Lu, J.; Sue Choi, J.; Lopata, V. *J. Compos. Mater.* **2005**, *39*, 1433.

28. Sui, G.; Zhong, W. H.; Yang, X. P. *Polym. Advan. Technol.* **2009**, *20*, 811.

29. Doring, M.; Arnold, U. *Polym. Int.* **2009**, *58*, 976.

30. Chen, J. H.; Johnston, A.; Petrescue, L.; Hojjati, M. *J. Appl. Polym. Sci.* **2009**, *111*, 2318.

31. Chen, J. H.; Johnston, A.; Petrescue, L.; Hojjati, M. *Radiat. Phys. Chem.* **2006**, *75*, 336.

32. Mascioni, M. Master thesis, Drexel University, **2002**.

33. Mascioni, M.; Ghosh, N. N.; Sands, J. M.; Palmese, G. R.; *J. Appl. Polym. Sci.* **2012** (DOI: 10.1002/APP.39189).